PNAS RESEARCH ARTICLE | NEUROSCIENCE

Histamine H_2 receptor deficit in glutamatergic neurons contributes to the pathogenesis of schizophrenia

Qianyi Ma[a,1], Lei Jiang[a,1], Han Chen[a], Dadao An[a], Yiting Ping[a], Yujia Wang[a], Haibin Dai[a], Xiangnan Zhang[a], Yi Wang[a,b], Zhong Chen[a,b,2], and Weiwei Hu[a,2]

Edited by Hee-Sup Shin, Institute for Basic Science, Daejeon, Korea (South); received April 25, 2022; accepted January 8, 2023

Schizophrenia is a serious mental disorder, and existing antipsychotic drugs show limited efficacy and cause unwanted side effects. The development of glutamatergic drugs for schizophrenia is currently challenging. Most functions of histamine in the brain are mediated by the histamine H_1 receptor; however, the role of the H_2 receptor (H_2R) is not quite clear, especially in schizophrenia. Here, we found that expression of H_2R in glutamatergic neurons of the frontal cortex was decreased in schizophrenia patients. Selective knockout of the H_2R gene (*Hrh2*) in glutamatergic neurons (*CaMKIIα-Cre; Hrh2*$^{fl/fl}$) induced schizophrenia-like phenotypes including sensorimotor gating deficits, increased susceptibility to hyperactivity, social withdrawal, anhedonia, and impaired working memory, as well as decreased firing of glutamatergic neurons in the medial prefrontal cortex (mPFC) in in vivo electrophysiological tests. Selective knockdown of H_2R in glutamatergic neurons in the mPFC but not those in the hippocampus also mimicked these schizophrenia-like phenotypes. Furthermore, electrophysiology experiments established that H_2R deficiency decreased the firing of glutamatergic neurons by enhancing the current through hyperpolarization-activated cyclic nucleotide-gated channels. In addition, either H_2R overexpression in glutamatergic neurons or H_2R agonism in the mPFC counteracted schizophrenia-like phenotypes in an MK-801-induced mouse model of schizophrenia. Taken together, our results suggest that deficit of H_2R in mPFC glutamatergic neurons may be pivotal to the pathogenesis of schizophrenia and that H_2R agonists can be regarded as potentially efficacious medications for schizophrenia therapy. The findings also provide evidence for enriching the conventional glutamate hypothesis for the pathogenesis of schizophrenia and improve the understanding of the functional role of H_2R in the brain, especially in glutamatergic neurons.

histamine H_2 receptor | glutamatergic neuron | HCN channel | medial prefrontal cortex | schizophrenia

Significance

Schizophrenia is a serious mental disorder, but there are still no satisfactory treatments. Currently, NMDA receptor-mediated glutamatergic transmission deficiency is thought to be the leading factor in the etiology of schizophrenia, but development of glutamatergic drugs is challenging. In the brain, most histamine functions are mediated by the H_1 receptor, and the role of the H_2 receptor (H_2R) is not quite clear, especially in schizophrenia. Our study demonstrates that functional deficiency of H_2R in mPFC glutamatergic neurons may be crucial for the pathogenesis of schizophrenia. H_2R in mPFC glutamatergic neurons may serve as a precise drug target, and H_2R agonists can be viewed as candidates for the treatment. Our study provides evidence for enriching the conventional glutamate hypothesis for schizophrenia and improves the understanding of the functional role of H_2R.

Schizophrenia is a serious mental disorder with a prevalence of about 1% in the population, making it a major socioeconomic problem. Schizophrenia is characterized by positive symptoms (including hallucinations, delusions, and disorganized behavior), negative symptoms (including social withdrawal, anhedonia, alogia, and blunted affect), and cognitive deficits. Hyperactivity of the dopaminergic system is considered to be a common cause of schizophrenia (1). Typical antipsychotic drugs antagonize the dopamine D_2 receptors; however, they often cause extrapyramidal side effects, and many individuals with negative symptoms seem refractory to them (2). Nontypical antipsychotics with complicated receptor-binding profiles do not adequately relieve both positive and negative symptoms, and they cause various unwanted effects, such as weight gain and sexual dysfunction (2, 3). Currently, a persistent defect in glutamatergic transmission involving NMDA receptors (NMDARs) is thought to be the leading factor in the etiology of schizophrenia, followed by dysfunction of the dopamine system (4, 5). Because of the toxicity of NMDAR agonists that directly act on the glutamate site, novel approaches to pharmacologically enhance the activity of NMDARs have been pursued. The effectiveness of agents binding to the glycine modulatory site and agonists of metabotropic glutamate receptors, which increase the function or expression of NMDARs, has been extensively investigated, but consistent efficacy in clinical trials has not been observed (6, 7). Gaining comprehensive insight into the pathophysiology of schizophrenia, especially the mechanisms pertinent to the glutamatergic system, may facilitate the development of promising and precise drug targets.

Histamine is an aminergic neurotransmitter involved in many pathophysiological processes including waking-sleeping, food intake, learning, and memory, and it primarily functions through the histamine H_1 receptor (H_1R) (8, 9). Elevated release and metabolism of histamine was found in the brains of schizophrenia patients (10), and we previously found that deficiency of H_1R in the basal forebrain cholinergic neurons induces behaviors

The authors declare no competing interest.

This article is a PNAS Direct Submission.

[1]Q.M. and L.J. contributed equally to this work.

[2]To whom correspondence may be addressed. Email: chenzhong@zju.edu.cn or huww@zju.edu.cn.

This article contains supporting information online at https://www.pnas.org/lookup/suppl/doi:10.1073/pnas.2207003120/-/DCSupplemental.

Published February 22, 2023.

resembling negative symptoms of schizophrenia, such as social withdrawal and anhedonia (11, 12). However, deficiency of H_1R in glutamatergic neurons or dopaminergic neurons did not lead to schizophrenia-like behaviors. Because the H_2 receptor (H_2R) is expressed as widely in the brain as H_1R, H_2R may also participate in brain functions involving histamine, such as the neuroendocrine regulation of pituitary hormone secretion release (13, 14) and memory consolidation (15–17). Our previous study revealed that H_2R retards the differentiation of oligodendrocytes following neonatal hypoxia-ischemia, suggesting a cell type-specific role of H_2R in brain disorders (18). Regarding schizophrenia, some clinical studies have offered preliminary evidence for the efficacy of H_2R antagonists as adjuvant treatments (19, 20), whereas a metaanalysis indicated that such therapy did not improve the overall symptoms of schizophrenia (21). Case–control studies have shown that schizophrenia patients have an elevated incidence of the $H_2R^{649}G$ allele for the H_2R gene *Hrh2*, which leads to a low level of downstream signaling (22, 23). This implies that H_2R may be linked to the pathogenesis of schizophrenia, but its effects are complicated. Since H_2R in different types of neurons may play diverse roles in brain disorders, the cell type-specific action of H_2R in schizophrenia is worth investigating.

In the present study, we specifically deleted *Hrh2* in glutamatergic neurons using the Cre-LoxP system and found that *CaMKIIα-Cre; Hrh2$^{fl/fl}$* mice displayed schizophrenia-like phenotypes, e.g., sensorimotor gating deficits, increased susceptibility to hyperactivity, social withdrawal, anhedonia, and impairment of working memory. The decreased firing of glutamatergic neurons in the medial prefrontal cortex (mPFC) due to H_2R deficiency and increased current through hyperpolarization-activated cyclic nucleotide-gated (HCN) channels are responsible for these behavioral deficits. We also verified that there is decreased histamine H_2R expression in glutamatergic neurons in schizophrenia patients. Finally, H_2R agonists reversed the schizophrenia-like behavior in MK-801-induced pharmacological models of schizophrenia, indicating that they hold great potential as a therapy for schizophrenia.

Results

Deficit of Histamine H_2R in Glutamatergic Neurons Causes Schizophrenia-Like Phenotypes. In an attempt to study the relationship of H_2R in glutamatergic neurons to schizophrenia, RNAscope in situ hybridization was carried out to determine the level of *Hrh2* mRNA in glutamatergic neurons of schizophrenia patients from the Netherlands Brain Bank (NBB) and Chinese Brain Bank (CBB) (*SI Appendix*, Table. S1). Compared with age-matched controls, schizophrenia patients had significantly lower *Hrh2* mRNA levels in the glutamatergic neurons in the frontal cortex, while the glutamate intensity and soma size of glutamatergic neurons remained unchanged (*SI Appendix*, Fig. S1 *A* and *B*). These results suggest that H_2R in glutamatergic neurons may participate in the pathogenesis of schizophrenia.

We then employed the Cre-LoxP system to selectively delete histamine *Hrh2* in forebrain glutamatergic neurons by crossing *CaMKIIα-Cre* mice with *Hrh2$^{fl/fl}$* mice (*SI Appendix*, Fig. S2*A*). The lack of H_2R expression in glutamatergic neurons in *CaMKIIα-Cre; Hrh2$^{fl/fl}$* mice was verified by an RNAscope assay (*SI Appendix*, Fig. S2 *B* and *C*). Examination of basic physiological functions revealed no significant differences in body temperature, pain sensitivity, hearing sensitivity, growth, or motor coordination between *CaMKIIα-Cre; Hrh2$^{fl/fl}$* mice and the control *Hrh2$^{fl/fl}$* and *CaMKIIα-Cre* mice (*SI Appendix*, Fig. S2 *D–H*). Prepulse inhibition (PPI) of the auditory startle reflex serves as an operational test of sensorimotor gating ability, and PPI deficits are often detected in individuals with schizophrenia (24, 25). We found that compared with control mice, *CaMKIIα-Cre; Hrh2$^{fl/fl}$* mice showed significantly lower PPI at 82 dB (Fig. 1*A*). In PPI tests, an increase in the percentage of PPI is reliably obtained with increasing prepulse intensity (26); however, *CaMKIIα-Cre; Hrh2$^{fl/fl}$* mice failed to show increased PPI at a stronger prepulse (82 dB, *SI Appendix*, Fig. S3*A*). In addition, we have also measured the prepulse-elicited reaction of mice and found that H_2R knockout in glutamatergic neurons did not affect startle-like reaction to prepulse stimulus (*SI Appendix*, Fig. S3 *C*). So, we proposed that H_2R knockout mice showed impaired sensory gating function. The results suggested that their perceived salience and/or processing of the prepulse stimulus appeared normal, while their attentional processing and modulation associated with pre-pulse inhibition showed defects, especially elicited by strong stimulus (26–28). Furthermore, risperidone, an antipsychotic drug, completely reversed the PPI deficit at 82 dB in *CaMKIIα-Cre; Hrh2$^{fl/fl}$* mice, but had no effects on control mice (*SI Appendix*, Fig. S4*A*). These results indicated that deficit of H_2R in glutamatergic neurons impairs the sensorimotor gating ability, and that this phenotype can be rescued by the antipsychotic drug risperidone.

Hyperactivity caused by the noncompetitive NMDAR antagonist MK-801 mimics the positive symptoms of schizophrenia (29). Here, we conducted an open-field test to evaluate the locomotor activity in mice given MK-801 or not. The results showed that locomotor activity was higher in *CaMKIIα-Cre; Hrh2$^{fl/fl}$* mice than that in control mice after MK-801 administration (Fig. 1*B1*), and this change could also be reversed by treatment with risperidone (Fig. 1 *B2* and *B3*). This suggests that loss of the histamine H_2R in glutamatergic neurons causes increased susceptibility to hyperactivity, which is associated with positive symptoms.

The negative symptoms in schizophrenia encompass social withdrawal and anhedonia. We conducted a three-chamber test and a nest building test to evaluate the social behaviors of the mice (Fig. 1 *C1–C3* and *D* and *SI Appendix*, Fig. S5 *A* and *B*). The three-chamber test comprises three phases: phase 1 for habituation, phase 2 for the evaluation of sociability to a stranger mouse, and phase 3 for the evaluation of social novelty recognition by introducing another stranger mouse (Fig. 1 *C1–C3*, and *SI Appendix*, Fig. S5 *A* and *B*). We found that there was no obvious preference for the left or right chamber between the *CaMKIIα-Cre; Hrh2$^{fl/fl}$* group and the control group during phase 1 (*SI Appendix*, Fig. S5*A*). During phase 2, mice in the control group showed a strong interest in the chamber where there was a stranger mouse (S1), whereas *CaMKIIα-Cre; Hrh2$^{fl/fl}$* mice did not show any preference (Fig. 1*C2*), indicating impaired sociability. During phase 3, a new stranger mouse was placed in another side of the chamber, but *CaMKIIα-Cre; Hrh2$^{fl/fl}$* mice still showed no preference for either of the two chambers (Fig. 1*C3*), suggesting reduced social novelty recognition. These results suggest that *CaMKIIα-Cre; Hrh2$^{fl/fl}$* mice display social indifference. We also noticed that the moved distance in the three-chamber test was higher for the *CaMKIIα-Cre; Hrh2$^{fl/fl}$* mice (*SI Appendix*, Fig. S5*B*), suggesting hyperlocomotion. In the nest building test, *CaMKIIα-Cre; Hrh2$^{fl/fl}$* mice had significantly lower nesting scores, and they used less cotton for nesting compared with control mice (Fig. 1*D*), which implies impaired social behavior. Next, we employed the sucrose preference test to detect anhedonia, the inability to experience pleasure from rewarding activities. *CaMKIIα-Cre; Hrh2$^{fl/fl}$* mice displayed a decreased preference for sucrose solution, while all groups drank an equal amount of total fluid (Fig. 1*E*). Furthermore, we found that the antipsychotic drug risperidone could rescue the social indifference and anhedonia of *CaMKIIα-Cre; Hrh2$^{fl/fl}$* mice, but not the loss of nest-building

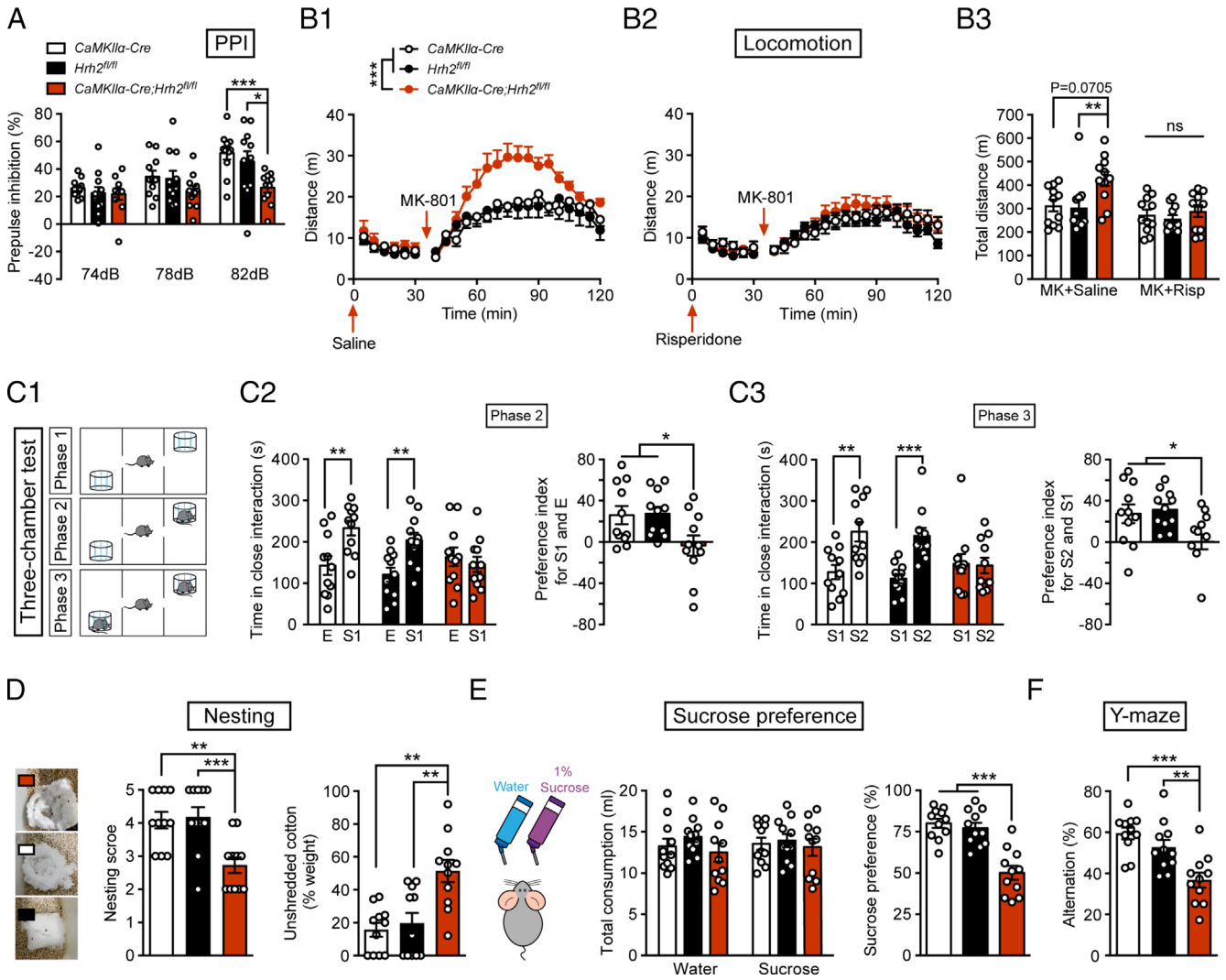

Fig. 1. Deficit of histamine H_2R expression in glutamatergic neurons induces schizophrenia-like phenotypes. (*A–F*) Sensorimotor gating ability, locomotion, social behavior, hedonic function, and cognitive behavior in *Hrh2*$^{fl/fl}$ (black), *CaMKIIα-Cre* (white), and *CaMKIIα-Cre; Hrh2*$^{fl/fl}$ (red) mice. (*A*) Sensorimotor gating ability assessed by percentage of PPI of the auditory startle reflex under 74, 78, and 82 dB prepulse intensities in startle tests. (*B1–B3*) Locomotion in an open-field test. (*B1*) Locomotor activity indicated by the distance traveled in the open field every 5 min. (*B2*) Locomotor activity indicated by the distance traveled in the open field every 5 min after the administration of risperidone. n = 11 mice for each group. (*B3*) The total distance traveled in the open field after administration of risperidone and MK-801. (*C1–C3*) Social behavior evaluated by the three-chamber test. E: metal cage with no mice in it; S1: a stranger mouse with the same gender; S2: another stranger mouse with the same gender. Risp: risperidone; MK: MK-801. (*C1*) Diagrammatic drawing of the three-chamber test. (*C2*) Time in close interaction (*Left*) and preference index for S1 and E (*Right*) during sociability testing (phase 2). (*C3*) Time in close interaction (*Left*) and preference index for S2 and S1 (*Right*) during social novelty recognition testing (phase 3). (*D*) Representative images (*Left*), nesting score (*Center*), and the percentage of the weight of unshredded cotton (*Right*) in a nest-building test. (*E*) Total consumption of water or sucrose (*Left*) and sucrose preference (*Right*) within 48 h. (*F*) Percentage of alternation in a Y-maze. n = 11 mice for each group. **P* ≤ 0.05, ***P* ≤ 0.01, ****P* ≤ 0.001. See also Dataset S1 for further statistical information.

function (*SI Appendix*, Fig. S4 *B–D*), which may be due to the suppression of locomotion and nestlet shredding by risperidone (30). Overall, the loss of H_2R in glutamatergic neurons in mice causes social withdrawal and an anhedonia-like state.

In addition to positive and negative symptoms, working memory deficits are also considered one of the major symptoms of schizophrenia (31). Here, we conducted the Y-maze test to evaluate the working memory of *CaMKIIα-Cre; Hrh2*$^{fl/fl}$ mice (Fig. 1*F*). The proportion of *CaMKIIα-Cre; Hrh2*$^{fl/fl}$ mice entering the correct arm was remarkably lower in comparison with that of control mice, and this effect could also be reversed by antipsychotic drug risperidone (*SI Appendix*, Fig. S4*E*). There was no difference in the total number of entries (26.64 ± 7.852 for *CaMKIIα-Cre* mice, 27.18 ± 10.11 for *Hrh2*$^{fl/fl}$ mice, and 25.27 ± 11.58 for *CaMKIIα-Cre; Hrh2*$^{fl/fl}$ mice), suggesting similar activity in Y-maze test. Together, the above results indicate that loss of histamine H_2R in glutamatergic neurons in mice results in schizophrenia-like phenotypes, namely sensorimotor gating deficits, increased susceptibility to hyperactivity, social withdrawal, anhedonia, and impaired working memory.

Deficit of H_2R in mPFC Glutamatergic Neurons Causes Schizophrenia-Like Phenotypes. Dysfunction of the glutamatergic system in the PFC and hippocampus is fundamental to the mechanism underlying the symptoms of schizophrenia, although the PFC and hippocampus may exhibit different abnormalities; for example, protein expression of the NMDAR subunit GluN1 in schizophrenia patients is higher or unchanged in the cortex, but lower in the hippocampus (32, 33). We thus selectively knocked down H_2R in the glutamatergic neurons in the mPFC and hippocampus by bilaterally injecting *AAV-FLEX-shHrh2-GFP* into the mPFC or hippocampus in *CaMKIIα-Cre* mice. In the mPFC, 83.75% of *CaMKIIα*-positive neurons coexpressed *GFP* and 100% of *GFP*-labeled neurons were positive for *CaMKIIα* (Fig. 2 *A* and

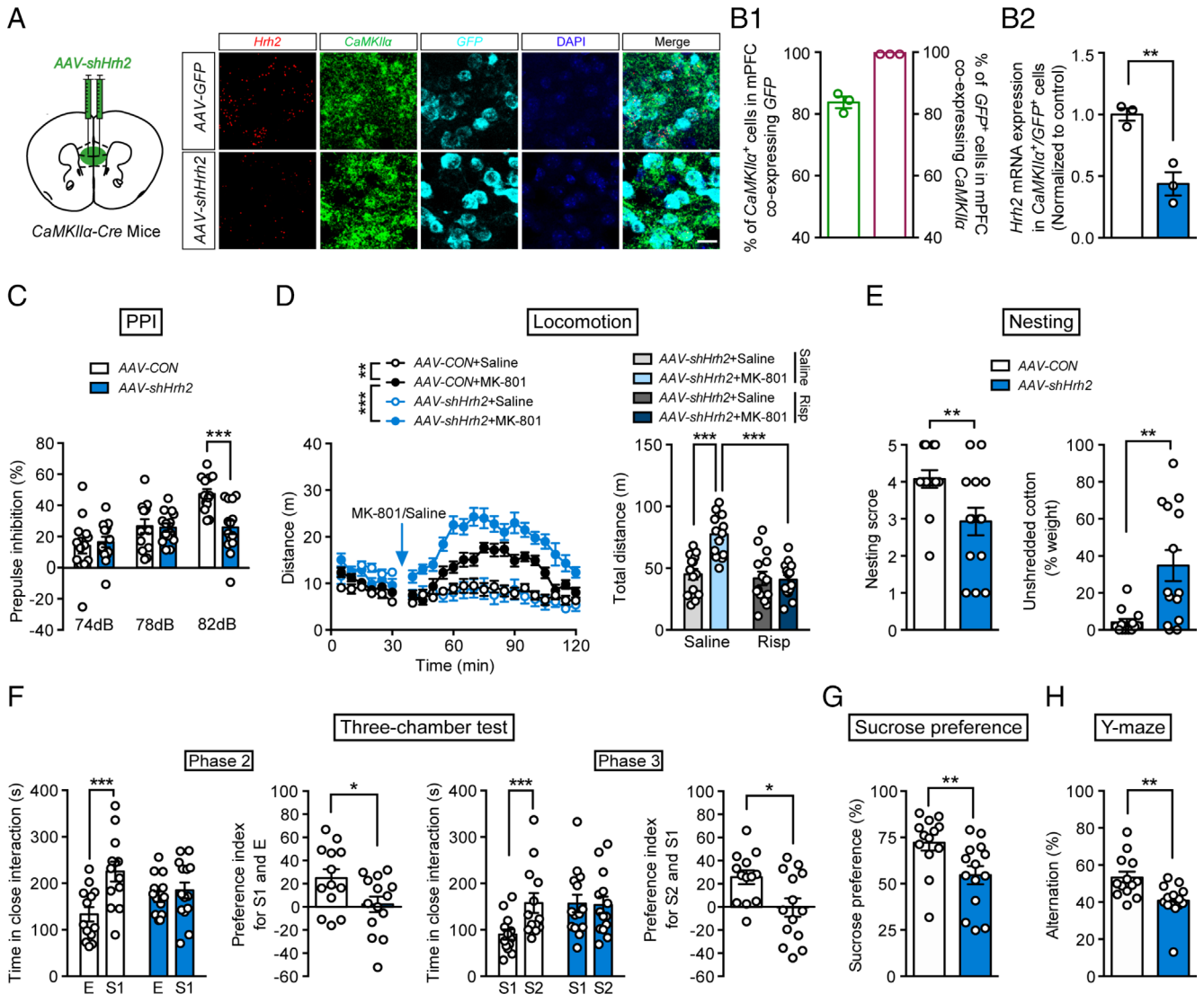

Fig. 2. Deficit of histamine H_2R in mPFC glutamatergic neurons induces schizophrenia-like behaviors. (*A*) Schematic diagram of the site of the injected virus (*Left*) and representative photographs of RNAscope assays of *Hrh2, CaMKIIα*, and *GFP* mRNA (*Right*). (Scale bar, 20 μm.) (*B1*) The percentage of *CaMKIIα*$^+$ glutamatergic neurons colabeled with *GFP* (*Left*), and the percentage of *GFP*$^+$ cells coexpressing *CaMKIIα* (*Right*). (*B2*) *Hrh2* expression in *CaMKIIα*$^+$/*GFP*$^+$ cells in *CaMKIIα-Cre* mice injected in the mPFC with *AAV-FLEX-scramble shRNA-GFP* (*AAV-CON*) or *AAV-FLEX-shHrh2-GFP* (*AAV-shHrh2*) to knock down H_2R. n = 3 mice. (*C–H*) Sensorimotor gating ability, locomotion, social behavior, hedonic function, and cognitive behavior in *CaMKIIα-Cre* mice injected in the mPFC with *AAV-CON* or *AAV-shHrh2*. (*C*) Percentage of PPI of the auditory startle reflex under 74, 78, and 82 dB prepulse intensities. (*D*) Distance traveled in the open field every 5 min (*Left*), and the total distance of *AAV-shHrh2* mice traveled in the open field (*Right*) after administration of MK-801 and risperidone in the first 30 min. For distance moved every 5 min, n = 14 *AAV-CON*+Saline; *AAV-CON*+MK-801 and *AAV-shHrh2*+Saline mice, n = 13 *AAV-shHrh2*+MK-801 mice. For total distance of *AAV-shHrh2* mice treated with risperidone and MK-801, n = 14 mice per group. (*E*) The nesting score (*Left*) and the percentage of the weight of unshredded cotton (*Right*) in a nest-building test. (*F*) Time in close interaction and preference index for a gender-matched stranger mouse (S1) and empty wire cage (E) in phase 2 and for another stranger mouse with the same gender (S2) and S1 in phase 3. (*G*) Sucrose preference within a 48-h period. (*H*) Percentage of correct alternation in the Y-maze. n = 13 for *CaMKIIα-Cre+AAV-CON* mice, and n = 14 for *CaMKIIα-Cre+AAV-shHrh2* mice. **P* ≤ 0.05, ***P* ≤ 0.01, ****P* ≤ 0.001. See also Dataset S1 for further statistical information.

B1). An RNAscope assay verified the low mRNA expression of H_2R in glutamatergic neurons after knockdown of H_2R in the mPFC (Fig. 2*B2*). We found that deficit of H_2R in the mPFC glutamatergic neurons led to behaviors resembling the symptoms of schizophrenia, namely deficits in PPI in a startle test, increased susceptibility to MK-801-induced hyperactivity in an open field, social withdrawal in a three-chamber test and nesting test, anhedonia in a sucrose preference test, and impaired working memory in a Y-maze test (Fig. 2 *C–H* and *SI Appendix*, Fig. S3 *B* and *D*, Fig. S5*D*). All of these schizophrenia-like behavioral impairments apart from the nesting-building deficit could be rescued by risperidone (*SI Appendix*, Fig. S5*E* and Fig. S6).

In the hippocampus, deficiency of H_2R expression was validated after transfection of *CaMKIIα-Cre* mice with *AAV-FLEX-shHrh2-GFP* (*SI Appendix*, Fig. S7 *A*, *B1*, and *B2*). However, knockdown of H_2R in the glutamatergic neurons in the hippocampus had no effect on sensorimotor gating ability, locomotion, social behavior, hedonic function, or working memory (*SI Appendix*, Figs. S5*F* and S7 *C–H*). These findings suggest that schizophrenia-like behavioral phenotypes result from H_2R dysfunction in the glutamatergic neurons in the mPFC instead of those in the hippocampus. In addition, the behavioral deficits in *CaMKIIα-Cre; Hrh2*$^{fl/fl}$ mice are not due to a developmental disorder, since postnatal knockdown of H_2R also produced schizophrenia-like phenotypes.

Overexpression of Histamine H_2R in mPFC Glutamatergic Neurons Improves Schizophrenia-Related Phenotypes. MK-801 can induce a full range of behavioral phenotypes related to schizophrenia, and it is often used for the evaluation of antipsychotic drugs (34). We found that there was a significant decrease in H_2R expression in mPFC

glutamatergic neurons after chronic administration of MK-801 for 2 wk (Fig. 3 *A1* and *A2*), suggesting that H_2R may contribute to the MK-801-induced schizophrenia-like phenotypes.

To further determine whether H_2R in glutamatergic neurons plays a role in schizophrenia-like phenotypes, *AAV-FLEX-Hrh2-GFP* was injected in *CaMKIIα-Cre* mice to overexpress H_2R in mPFC glutamatergic neurons, and then mice were exposed to MK-801. An RNAscope assay validated the successful expression of H_2R in mPFC glutamatergic neurons (Fig. 3 *B* and *C*). We found that MK-801 induced behavioral deficits, namely dysfunction in sensorimotor

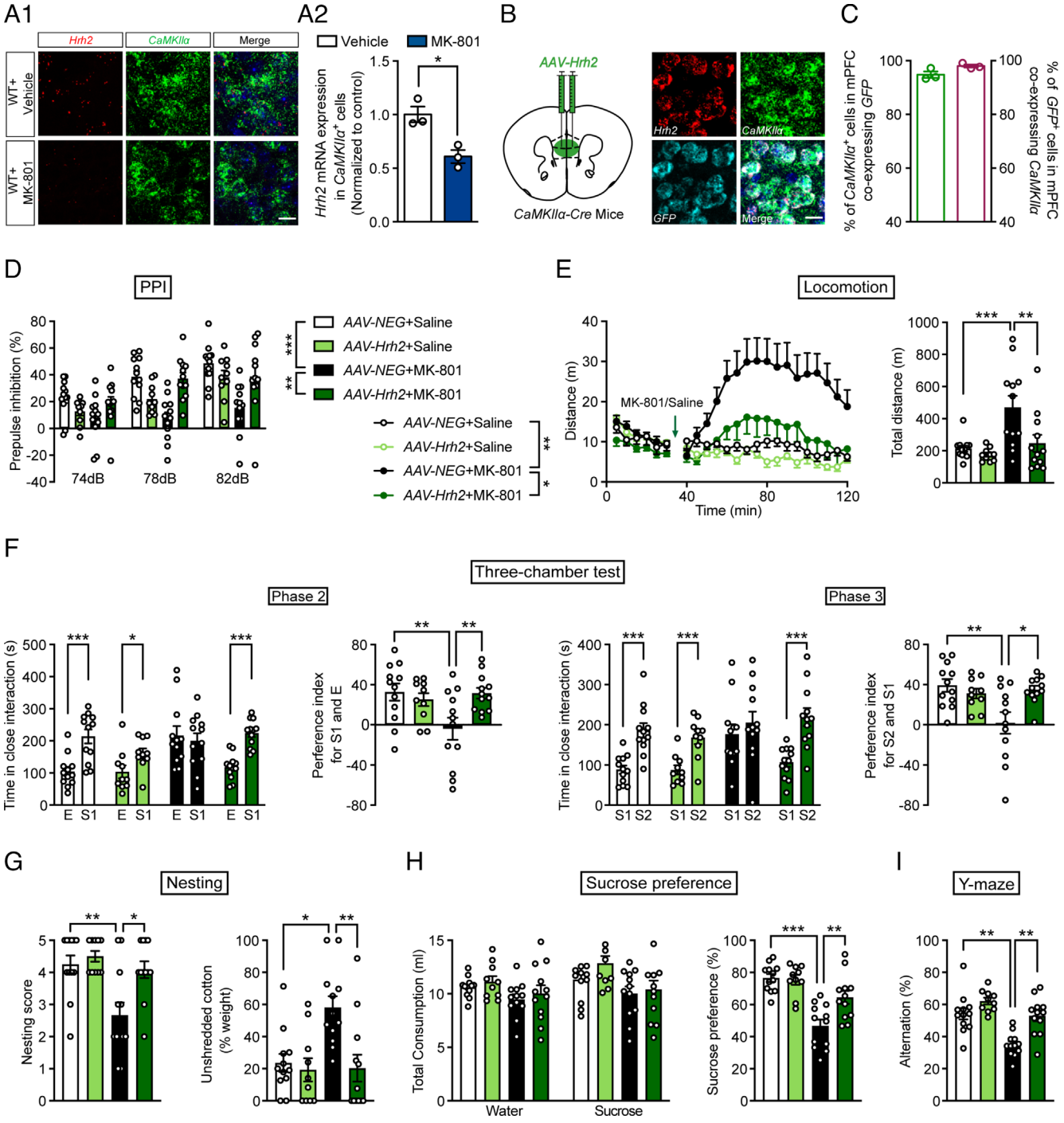

Fig. 3. Overexpression of histamine H_2R in mPFC glutamatergic neurons rescues schizophrenia-like behaviors induced by MK-801. (*A1*) Diagrammatic drawing of *Hrh2* and *CaMKIIα* mRNA expression in the mPFC of WT mice after the administration of vehicle or MK-801. (*A2*) *Hrh2* mRNA in *CaMKIIα*$^+$ cells was quantified. (Scale bar, 20 μm.) (*B*) Schematic diagram of the location of the injected virus (*Left*) and representative photographs of RNAscope in situ hybridization assays of *Hrh2, CaMKIIα*, and *GFP* mRNA (*Right*). (Scale bar, 20 μm.) (*C*) The percentage of *CaMKIIα*$^+$ glutamatergic neurons colabeled with *GFP* (*Left*) and the percentage of *GFP*$^+$ cells coexpressing *CaMKIIα* (*Right*). n = 3 mice. (*D–I*) Sensorimotor gating ability, locomotion, social behavior, hedonic function, and cognitive behavior of *CaMKIIα-Cre* mice infected with *AAV-FLEX-neg-GFP* (*AAV-NEG*, control) or with *AAV-FLEX-Hrh2-GFP* (*AAV-Hrh2*) to overexpress H_2R in the mPFC after MK-801 administration. (*D*) Percentage of PPI of the auditory startle reflex under 74, 78, and 82 dB prepulse intensities. (E) Distance traveled in the open field every 5 min (*Left*) and the total distance traveled in the open field (*Right*). (*F*) Time in close interaction and preference index for a gender-matched stranger mouse (S1) and empty wire cage (E) in phase 2 and for another new stranger mouse with the same gender (S2) and S1 in phase 3. (*G*) Nesting score (*Left*) and percentage of the weight of unshredded cotton (*Right*) in a nest-building test. (*H*) Sucrose preference within 48 h. (*I*) Percentage of correct alternation in a Y-maze. n = 12 for *CaMKIIα-Cre+AAV-NEG*+Saline mice, n = 12 for *CaMKIIα-Cre+AAV-NEG*+Saline mice, n = 12 for CaMKMK-801 mice, n = 10 for *CaMKIIα-Cre+AAV-Hrh2*+Saline mice, and n = 12 for *CaMKIIα-Cre+AAV-Hrh2*+MK-801 mice. *$P \le 0.05$, **$P \le 0.01$, ***$P \le 0.001$. See also Dataset S1 for further statistical information.

gating function, hyperactivity, social withdrawal, anhedonia, and impaired working memory, all of which could be recovered by overexpression of H_2R in mPFC glutamatergic neurons (Fig. 3 *D–I* and *SI Appendix*, Fig. S5*G*). In contrast, overexpression of H_2R in control mice had no effect on behaviors related to schizophrenia. These data further support the hypothesis that H_2R in mPFC glutamatergic neurons contributes to the pathogenesis of schizophrenia.

Deficit of H_2R in mPFC Glutamatergic Neurons Reduces Neuronal Activity. Neuronal activity and signal transmission are often compromised in schizophrenia; therefore, extracellular recording of glutamatergic neuron firing was performed in *CaMKIIα-Cre; Hrh2$^{fl/fl}$* mice. The results showed that there was a decrease in the firing of mPFC glutamatergic neurons in *CaMKIIα-Cre; Hrh2$^{fl/fl}$* mice compared with *Hrh2$^{fl/fl}$* control mice (Fig. 4 *A* and *B1*). Bursts are more effective than single spikes at enhancing neurotransmitter release and signal transmission, and a reduced burst is linked to schizophrenia (35). We found that bursts per minute and percentage of spikes per bursts were lower in *CaMKIIα-Cre; Hrh2$^{fl/fl}$* mice compared with *Hrh2$^{fl/fl}$* control mice (Fig. 4*B2*), suggesting that H_2R deficiency attenuates neuronal activity and signal transmission efficiency in the mPFC, which could compromise mPFC function in the organization of behavior.

We next examined the activity of mPFC glutamatergic neurons with knockdown of H_2R using whole-cell patch-clamp recording (Fig. 4*C*). There was no significant difference in action potential properties, namely the injected current for the first action potential, action potential threshold, and amplitude (Fig. 4 *D–F*). However, these neurons showed a reduced frequency of evoked action potentials, indicating decreased neuronal activity (Fig. 4 *G–H*), which is consistent with the reduced firing observed in vivo.

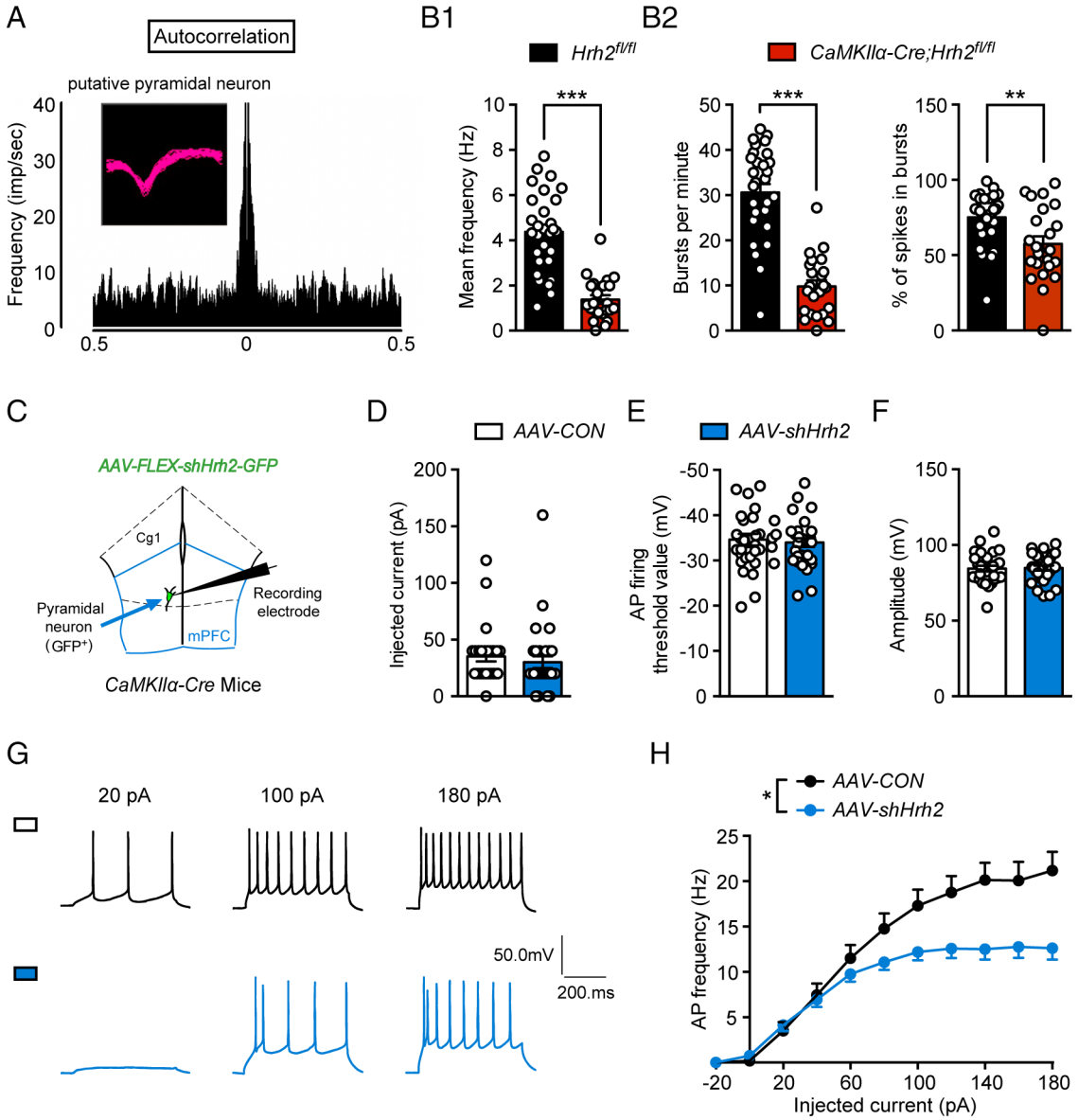

Fig. 4. Deficit of H_2R causes decreased activity of glutaminergic neurons. (*A*) Spike waveforms and autocorrelation of putative pyramidal neurons. (*B1*) Mean firing frequency of glutamatergic neurons in the mPFC of *Hrh2$^{fl/fl}$* and *CaMKIIα-Cre; Hrh2$^{fl/fl}$* mice. (*B2*) Burst per minute (*Left*) and percentage of spikes in bursts (*Right*) in the mPFC of *Hrh2$^{fl/fl}$* and *CaMKIIα-Cre; Hrh2$^{fl/fl}$* mice. n = 29 cells from three *Hrh2$^{fl/fl}$* mice, n = 23 cells from three *CaMKIIα-Cre; Hrh2$^{fl/fl}$* mice. (*C–H*) Patch-clamp recordings of glutamatergic neurons from *CaMKIIα-Cre* mice injected in the mPFC with *AAV-FLEX-scramble shRNA-GFP* (*AAV-CON*) or *AAV-FLEX-shHrh2-GFP (AAV-shHrh2)*. (*C*) A schematic diagram demonstrating recordings of mPFC glutamatergic neurons. (*D–F*) Action electrical properties, namely (*D*) the injected current inducing the first action potential (AP), (*E*) AP firing threshold, and (*F*) AP amplitude. (*G*) Representative AP firing patterns. (*H*) Frequency of APs evoked by injected currents from −20 to 180 pA. n = 29 cells from five *CaMKIIα-Cre+ AAV-CON* mice, n = 32 cells from six *CaMKIIα-Cre+AAV-shHrh2* mice. $^{**}P \le 0.01$, $^{***}P \le 0.001$. See also Dataset S1 for further statistical information.

Deficit of H_2R Enhances HCN Channel Activity in Glutamatergic Neurons and Provokes Schizophrenia-Like Behaviors. Hyperpolarization-activated current I_h mediated by HCN channels is critical to controlling neuronal activity (36, 37). We found that the amplitude of the I_h current was remarkably higher in mPFC glutamatergic neurons lacking H_2R (Fig. 5 *A, B1*, and *B2*). To further confirm whether increased current through HCN channels is related to the dysfunction of mPFC glutamatergic neurons lacking H_2R, we recorded the evoked action potential frequency after administration of ZD7288, a specific HCN channel blocker. We found that ZD7288 completely rescued the reduced activity of mPFC glutamatergic neurons lacking H_2R, but had no effects in controls (Fig. 5*C*). The above results implied that the deficit of H_2R decreased the firing of glutamatergic neurons by enhancing current through HCN channels.

To further test the hypothesis that the schizophrenia-like phenotypes induced by H_2R deficit in mPFC glutamatergic neurons were due to the increase of the I_h current, we infused ZD7288 into the mPFC of *CaMKIIα-Cre* mice infected with *AAV-shHrh2* (Fig. 5*D*). The results showed that ZD7288 was able to rescue the schizophrenia-related behavioral deficits, namely impaired sensorimotor gating function, increased sensitivity to MK-801, and

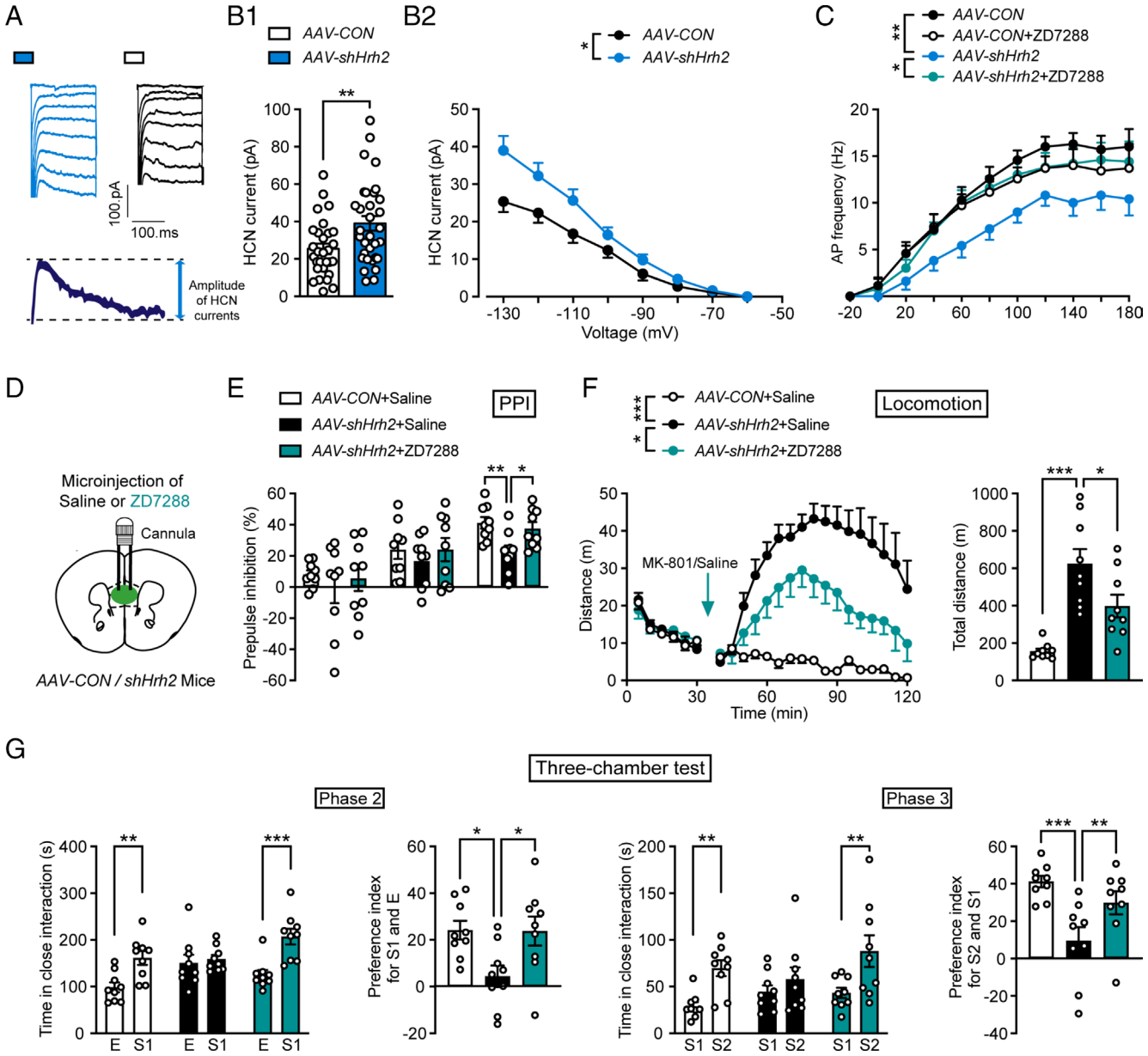

Fig. 5. H_2R knockdown causes neuronal hypoactivity *via* enhancement of HCN I_h currents, and blocking HCN rescues schizophrenia-like phenotypes. (*A*) Representative hyperpolarization-activated I_h currents mediated by HCN channels. I_h (HCN current) was calculated by measuring the amplitude of current generated at voltages from −60 mV to −130 mV for 200 ms, with 10 mV increments. (*B1*) HCN currents evoked by −130 mV and (*B2*) by hyperpolarizing 20 mV steps from −130 mV to −60 mV. n = 29 cells from five *CaMKIIα-Cre+AAV-FLEX-scramble shRNA-GFP* mice (*AAV-CON*), n = 32 cells from six *CaMKIIα-Cre+AAV-FLEX-shHrh2-GFP* mice (*AAV-shHrh2*). (*C*) AP frequency after incubation with 50 μM ZD7288. n = 7 cells from four *CaMKIIα-Cre+AAV-CON* mice, n = 10 cells from five *CaMKIIα-Cre+AAV-shHrh2* mice. (*D*) Abridged general view of the position of the cannula. (*E–G*) Sensorimotor gating ability, locomotion, and social behavior of *CaMKIIα-Cre* mice infected with *AAV-CON* or *AAV-shHrh2* in the mPFC and then treated with saline or the HCN inhibitor ZD7288. n = 9 mice for each group. (*E*) Percentage of PPI of the auditory startle reflex under 74, 78, and 82 dB prepulse intensities. (*F*) Distance traveled in the open field every 5 min (*Left*) and the total distance traveled in the open field (*Right*) after administration of MK-801. (*G*) Social behavior evaluated by a three-chamber test. Time in close interaction and preference index for S1 and E in phase 2 and for S2 and S1 in phase 3. $^*P \le 0.05$, $^{**}P \le 0.01$, $^{***}P \le 0.001$. See also Dataset S1 for further statistical information.

social indifference (Fig. 5 *E–G* and *SI Appendix*, Fig. S5*H*). Together, these results suggest that H_2R deficit reduces the activity of mPFC glutamatergic neurons by upregulating HCN channel current and triggers schizophrenia-like behavioral phenotypes.

H_2R Agonists Improve Behavioral Phenotypes Related to Schizophrenia. To explore whether H_2R agonists can be used for the treatment of schizophrenia, we injected amthamine or betazole into the mPFC and evaluated MK-801-induced behavioral deficits (Fig. 6*A*). Amthamine is a highly selective histamine H_2R agonist, which does not stimulate the H_1 and H_3 receptors, and betazole also activates H_2R and is used for diagnostic applications in clinic (38, 39). We found that both amthamine and betazole alleviated all schizophrenia-related behavioral disorders (impaired sensorimotor gating, increased susceptibility to MK-801-induced hyperactivity, social withdrawal, and anhedonia), except for impaired working memory Fig. 6 *B–G* and *SI Appendix*, Fig. S5*I*).

We then recorded the electrical properties of glutamatergic neurons in the mPFC after H_2R agonist treatment by whole-cell patch clamping. The data showed that amthamine reversed the reduced neuronal activity and the increased HCN channel-mediated I_h current of glutamatergic neurons after MK-801 administration, while the action potential properties were unchanged (Fig. 6 *H–N*). These results suggest that H_2R agonists relieve schizophrenia-like behaviors by acting on HCN channels in an experimental schizophrenia model.

Discussion

Although H_2R was identified in the brain decades ago, its function is still largely unknown. Our recent studies indicate that H_2R expression in oligodendrocytes impedes their differentiation and remyelination (18), while H_2R expression in neural stem cells is not involved in their differentiation and neurogenesis following brain injury (40). This highlights the complicated role of H_2R in brain disorders, in which its actions depend on the type of neuron. In the present study, we found that a deficit of H_2R in glutamatergic neurons was sufficient to produce several behavioral and pathophysiological characteristics in mice that resemble human schizophrenia. *CaMKIIα-Cre; Hrh2*$^{fl/fl}$ mice showed both positive symptom-related behaviors, such as a high susceptibility to hyperactivity, and negative symptom-related behaviors, such as deficits in sociability, social novelty recognition, and nesting, which mirror social withdrawal, and a reduced preference for a sweet solution, which mirrors anhedonia. Moreover, these mice also showed cognitive symptoms such as working memory deficits, which are also a core feature of schizophrenia (31). Sensorimotor gating is usually compromised in schizophrenia patients and is associated with neurocognitive functional status (24). This deficit was observed in the *CaMKIIα-Cre; Hrh2*$^{fl/fl}$ mice as indicated by decreased PPI in startle tests. Above abnormal behaviors were rescued by the antipsychotic drug risperidone, which normalizes the extracellular glutamate level in schizophrenia models (41). Importantly, we observed a decrease of H_2R expression in glutamatergic neurons in individuals with schizophrenia compared with the age-matched control. Selective knockdown of H_2R expression in glutamatergic neurons also resulted in a collection schizophrenia-like behavioral features, whereas overexpression of H_2R reversed the psychotic symptoms in an MK-801-induced animal model of schizophrenia. Our study provides strong experimental evidence for the hypothesis that H_2R deficit in glutamatergic neurons is a primary cause of schizophrenia pathogenesis.

The glutamate hypothesis has exerted a great influence on schizophrenia research and the discovery of novel treatments (5, 7). Although numerous schizophrenia susceptibility genes connected with glutamate transmission have been identified (42), the molecular mechanism underlying the dysfunction in glutamatergic neurons is still unclear. Taking account the findings of this study together with those of our previous study (11), we propose that H_2R, but not H_1R, in glutamatergic neurons contributes to the pathogenesis of schizophrenia. This critical role of H_2R in glutamatergic neurons in schizophrenia enriches the theory of conventional glutamate hypothesis for schizophrenia, and also improves the understanding of functional role of H_2R in brain disorders. Importantly, H_2R in glutamatergic neurons could serve as a precise drug target for the treatment of schizophrenia. Besides, genetic animal models related to glutamatergic transmission have been proposed for schizophrenia, but they may have some limitations (43). For example, Grin1^{D481N} mice with a robust decrease in NMDAR glycine affinity show impairments in sociability and cognition, but lack psychotic features; Grin1$^{D481N/K483Q}$ mice, which have two-point mutations in the D-serine/glycine site of NMDAR, are resistant to antipsychotics (44, 45). Our study revealed that the phenotype of mice with a deficit of H_2R in mPFC glutamatergic neurons is associated with all the symptoms of schizophrenia, which can be reversed by antipsychotics. So, it may serve as an animal model for pathogenic research or drug development for schizophrenia.

The glutamate hypothesis postulates the disruption of neural pathways through NMDAR hypofunction (4, 7). It has been suggested that deficiency of NMDAR in interneurons in the PFC or hippocampus leads to reduced inhibitory GABA neurotransmission, which produces "noise" that impairs filtering of irrelevant information and information processing (35). In addition, both the PFC and hippocampus are often compromised in models of genetic risk of schizophrenia, such as 22q11.2 microdeletion, DISC1 mutations, and parvalbumin interneuron-specific knockout of ERbB4. Our study demonstrated that *Hrh2* deletion in the glutamatergic neurons of the mPFC, but not those in the hippocampus, leads to the schizophrenia-like behaviors. So, it is enticing to speculate that the dysfunction of mPFC glutamatergic neurons caused by H_2R deficit, rather than the complete dysfunction of both interneurons and pyramidal neurons or of both the PFC and hippocampus, is sufficient to produce behavioral changes associated with schizophrenia. This idea is supported by the evidence that deletion of NMDAR subunit NR1 in forebrain pyramidal neurons causes schizophrenia-like behavioral phenotypes (46). In addition, we noticed that the deletion of H_2R in glutamatergic neurons reduced their activity and burst firing, which could decrease the "signal" and thus lower the "signal-to-noise ratio" and then diminish the ability of these neurons to encode information. In contrast to our observation, forebrain pyramidal cell-specific NR1 knockout mice displayed increased pyramidal cell excitability but decreased evoked gamma band oscillatory activity (46, 47). This increased ratio of excitation to inhibition, which could result in elevated "noise," was also observed in genetic models for schizophrenia, such as mice with mutation of DISC1, or overexpression of D_2 receptors (48). We propose that the alteration of "signal" and "noise," regardless of bias toward increased "noise" or decreased "signal," could be translated into a reduction in firing bursts that attenuates signal transmission efficiency and serves as a critical pathogenic cause of schizophrenia.

Furthermore, we found that H_2R deficit reduced neuronal firing through the elevation of current through HCN channels, while H_2R agonists enhanced neuronal excitability through reduction of HCN channel current. HCN channels serve as the targets of various cellular signals that fine tune neuronal responses to external stimuli (37). HCN channels mediate hyperpolarization-activated I_h currents, which play a key role in the modulation of neuronal activity and synaptic transmission (36, 37). However, it has been reported that H_2R activation can increase the HCN channel-mediated I_h

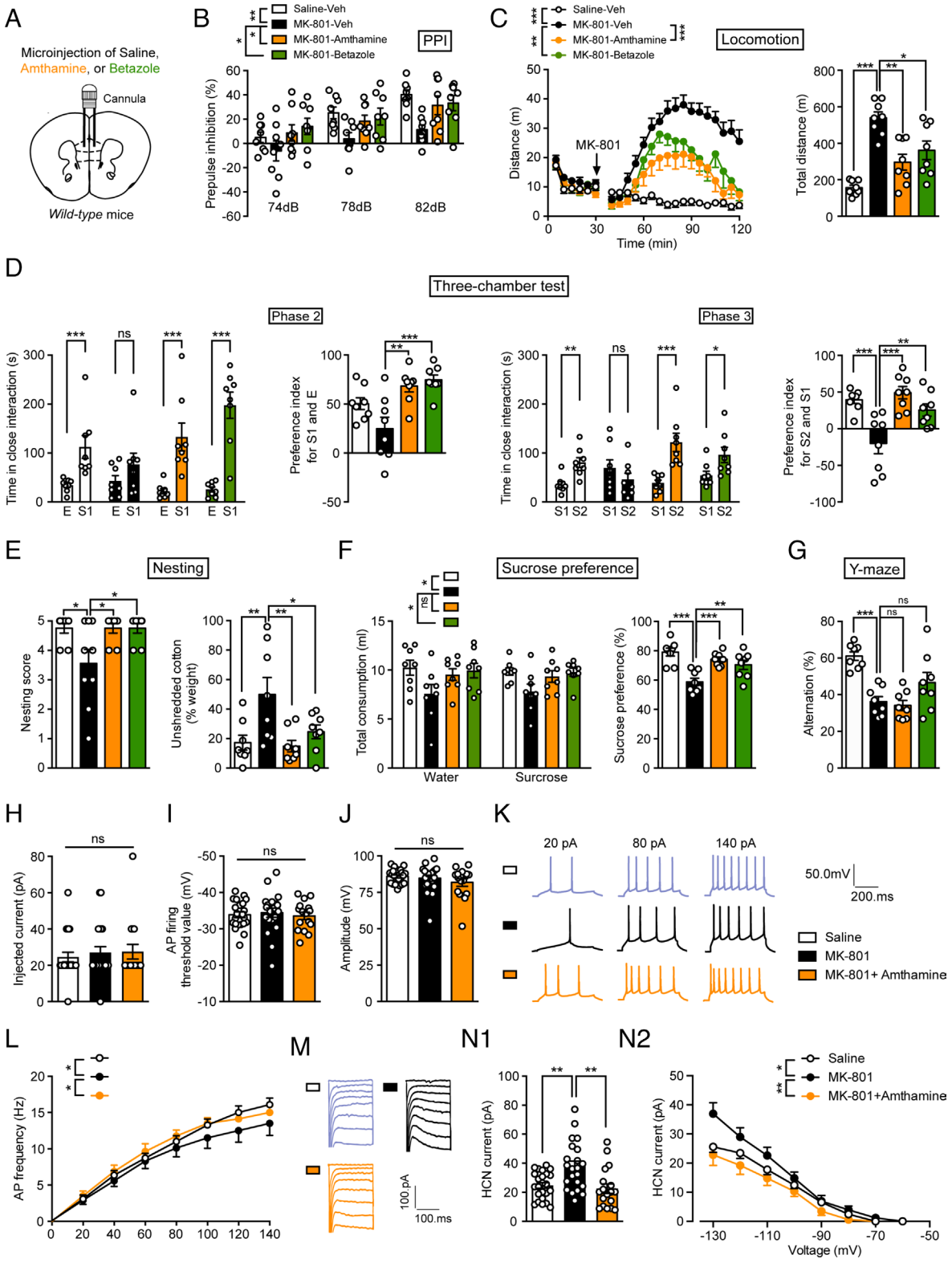

Fig. 6. Histamine H_2R agonists rescue schizophrenia-like behaviors induced by MK-801. (*A*) Abridged general view of the position of the cannula. (*B–G*) Sensorimotor gating ability, locomotion, social behavior, hedonic function, and cognitive behavior of WT mice treated with saline, amthamine, or betazole after chronic exposure to MK-801. n = 8 mice for each group. (*B*) Percentage of PPI of the auditory startle reflex under 74, 78, and 82 dB prepulse intensities. (*C*) Distance traveled in the open field every 5 min (*Left*) and the total distance traveled in the open field (*Right*). (*D*) Time in close interaction and preference index for a gender-matched stranger mouse (S1) and empty wire cage (E) in phase 2 and for a new gender-matched stranger mouse (S2) and S1 in phase 3. (*E*) The nesting score (*Left*) and the percentage of the weight of unshredded cotton (*Right*) in a nest-building test. (*F*) Total consumption of water or sucrose (*Left*) and the sucrose preference (*Right*) within a 48-h period. (*G*) Percentage of correct alternation in a Y-maze. (*H–N*) The electrophysiological properties of mPFC glutamatergic neurons in WT mice treated with saline, MK-801, or MK-801 combined with amthamine. (*H–J*) Action potential (AP) properties, namely (*H*) the injected current inducing the first AP, (*I*) AP firing threshold, and (*J*) AP amplitude for three groups of mice. (*K*) Representative AP firing patterns in mPFC glutamatergic neurons. (*L*) Frequency of APs in mPFC glutamatergic neurons evoked by injected currents ranging from 0–140 pA. (*M*) Representative hyperpolarization-activated I_h currents mediated by HCN channels in mPFC glutamatergic neurons. (*N1*) HCN current evoked by −130 mV and (*N2*) by hyperpolarizing 20 mV steps from −130 mV to −60 mV. n = 24 cells from four saline mice, n = 22 cells from six MK-801 mice, n = 18 cells from five saline+amthamine mice. See also Dataset S1 for further statistical information.

current to excite subthalamic nucleus neurons (49, 50). These inconsistent actions of H_2R on HCN channels could be due to differences in neuron subtypes or different downstream signaling pathways. Nevertheless, the regulation of HCN channels is involved in the action of H_2R in maintaining mPFC glutamatergic neuron activity, information processing, and behavior organization.

Developing glutamatergic drugs for schizophrenia has proved to be extremely challenging. Although some studies indicated the beneficial effects of increasing NMDAR activation through the use of drugs acting on the glycine modulatory site, larger trials did not demonstrate the efficacy of these drugs (6, 7). At high doses, D-cycloserine, an NMDAR glycine site partial agonist, even worsens positive symptoms, probably because it competes with endogenous glycine at high doses (51). The glycine transporter inhibitor bitopertin and the mGluR2/3 agonist pomaglumetad methionil also failed in Phase III clinical trials, showing no significant benefit in treating clinical symptoms (52–54). Therefore, it is necessary to identify other glutamate-acting drugs for future therapies. Since betazole has been used for diagnostic applications to test gastric acid secretion in clinic, it has had a favorable safety profile, which has encouraged its further application in the treatment of schizophrenia. Our previous study suggested that H_1R deficiency in cholinergic neurons may serve as a drug target specific to negative symptoms of schizophrenia (11). Therefore, H_1R and H_2R ligands may be suitable for patients with different symptoms. Nevertheless, H_2R agonists hold great potential as they may cover both the positive and negative symptoms of schizophrenia and may be feasible for direct clinical application. Moreover, there is evidence of H_2R antagonist famotidine augmentation of antipsychotic medications in schizophrenia patients, but some randomized controlled trials of famotidine did not show consistent efficacy in treating the symptoms of schizophrenia (55–58). Some evidence suggests that the benefits of famotidine for schizophrenia may not arise from H_2R antagonism (11, 59).

Taken together, our results suggest that deficit of H_2R in mPFC glutamatergic neurons may be pivotal to the pathogenesis of schizophrenia and that it could be viewed as a new drug target. Our findings provide evidence for enriching the conventional glutamate hypothesis for the pathogenesis of schizophrenia and highlight the fact that H_2R agonists can serve as drug candidates for schizophrenia therapy. They also improve the understanding of the functional role of H_2R in the brain, especially in glutamatergic neurons.

Materials and Methods

Animals. *Hrh2*$^{fl/fl}$ mice were generated by the Nanjing Biomedical Research Institute of Nanjing University, Nanjing, China. *Hrh2*$^{fl/fl}$ homozygous mice were crossed with *CaMKIIα-Cre* mice (Jax No. 005359) in order to specifically delete *Hrh2* in *CaMKIIα*+ glutamatergic neurons. All mice were maintained in a C57BL/6J genetic background. Mice were raised and used according to the guidelines of the Animal Advisory Committee of Zhejiang University and the US NIH Guidelines for the Care and Use of Laboratory Animals. All procedures were approved by the Animal Advisory Committee of Zhejiang University.

For genotyping *Hrh2*$^{fl/fl}$ mice the oligos Hrh2-loxptF (5′-CTTGTGGAGGTG ATCTGGTGA-3′) and Hrh2-loxptR (5′-CGCCCATGTCTAAGCGTTAT-3′) were used; the PCR products were 299 bp [wild-type (WT) allele] and 417 bp (floxed allele). The program was 95 °C, 5 min; 95 °C, 30 s, 58 °C, 30 s, and 72 °C, 30 s (40×); and 72 °C, 5 min. For genotyping of *CaMKIIα-Cre* mice, the oligos Cre-f2 (5′-TGCCCAAGAAGAAGAGGAA-3′) and Cre-r2 (5′-TTGCAGGTACAGGAGGTAGTC-3′) were used; the PCR products were 200 to 250 bp (positive allele). The program was 94 °C, 3 min; 95 °C, 30 s, 58 °C, 30 s, and 72 °C, 30 s (35×); and 72 °C, 2 min.

Postmortem Brain Material. Human postmortem brain tissues were acquired from the China Brain Bank (CBB, No. S2019002) and NBB (No. 2017-1164). Written consent for the use of brain samples from the CBB was obtained from all the participants according to the standardized operational protocol for human brain banking in China (60), and written consent for the brain samples from the NBB for brain autopsy and the use of the material and clinical information for research purposes were obtained by the NBB. We obtained tissues from five schizophrenia patients and five controls each from CBB and NBB. Controls had no reports of dementia or mental disorders. Sex, age, postmortem delay, cerebrospinal fluid pH, brain weight, and Braak stage of Alzheimer pathology were matched between schizophrenia patients and controls. All experimental procedures were in accordance with the guidelines for the conduct of research involving human subjects as established by the Ethics Committee of Zhejiang University School of Medicine. All protocols were approved by the Ethics Committee of Zhejiang University School of Medicine. Detailed clinicopathological information is shown in Supplemental *SI Appendix*, Table S1.

Behavior Assays. Mice aged 8 to 14 wk were employed for all behavioral experiments. The mice were habituated in the testing room for at least 30 min in advance. All behavioral tasks were conducted during the daytime. To avoid the influence of odor during the test, the excreta of the mice were cleaned after each test, and the apparatus was cleaned with 70% ethanol to eliminate the odor from the mice. All behavioral tests were performed following protocols published previously (11).

Body Temperature Test. Before each measurement, the mercury column of the anal thermometer was adjusted to below 35 °C to ensure the accuracy of temperature measurement. The bottom of the anal thermometer was smeared with an appropriate amount of liquid paraffin to ensure smooth insertion. Mice were grabbed and the anal thermometer inserted into their anus at a consistent depth. After measuring, the anal thermometer was wiped with alcohol before the next measurement.

Hot Plate Test. Room temperature was controlled at about 25 °C to avoid the influence of external temperature during the test. When mice were stimulated by heat, they felt pain and showed symptoms such as licking of the hind paw, lifting of the hind paw, and twisting of the waist. We used licking of the hind paw as an indicator of pain sensation. The mice were placed gently on a hot plate (55 ± 0.1 °C), and the latency in time to response (licking of the hind paw) was recorded. After the measurement, the mice were removed from the hot plate at once and sent to their homecage to rest.

Hearing Test. The mice were placed gently in the test chamber and habituated for 5 min. Later, each mouse was subjected to a startle stimulus (120 dB, 40 ms), and the startle amplitude was evaluated to measure the hearing of the mouse.

Accelerating Rotarod. Mice were gently placed on an accelerating rotarod (YLS-4C, ShangHai Biowill, China), which was about 6 cm wide, 3 cm in diameter, and elevated at a height of 35 cm. The speed of the apparatus was initially 5 rpm and increased gradually to 40 rpm. The time interval from the mouse just being placed on the rod to falling off the rod was recorded. When the mouse did not fall off of the rod within 5 min, the experiment was stopped and the latency was recorded as 5 min. Each mouse was tested eight times, with at least 20 min between each test.

PPI. The PPI test was carried out in SR-LAB startle chambers. The mice were confined to the test chamber and acclimated to the environment with background white noise of 70 dB for 5 min, followed by five 20-ms startle pulses of 120 dB. After that the mice were delivered six sets of tests, each consisting of eight different stimulus types in a pseudorandom distribution: no stimulus, startle tone only, pulse tone only (74, 78, or 82 dB), pulse paired with a startle tone, and a block of five 20-ms 120-dB startle pulses. The maximum amplitude of the startle response of the mice under each type of trial was recorded and the average of the six tests was used for data analysis. PPI% = [(1- average response to prepulse before startle stimulus/average response to startle stimulus)] ×100

Open-Field Test. An open square box (45 cm × 45 cm × 45 cm) was used for the open-field test. The mice were placed in the center of the box in a specific direction and were permitted to freely explore the box for 2 h. Automatic video tracking (ANY-maze) was used to automatically track the movement, and the total distance and the distance traveled per 5 min were analyzed.

Three-Chamber Test. The device for the three-chamber test was made up of a plexiglass box (60 cm × 40 cm × 20 cm) with a partition dividing the box into three rectangular chambers and a small door on the partition allowing the mice to move freely. The test was divided into three phases: A) Habituation (phase 1), in which a metal wire cage was placed in left and right chambers, and the test mice were placed in the middle chamber and permitted to explore freely for 10 min.

The total time the mice spent in each chamber was used as a measure of their preference for each chamber. B) Sociability (phase 2), in which a weight- and gender-matched stranger mouse (S1) was put into the metal cage in the left or right chamber. The test mouse was introduced into the middle chamber and permitted to move freely. The times spent in close interaction with the empty cage and the cage with the S1 mouse were recorded to determine the sociability of the test mouse. C) Social novelty (Phase 3), in which another novel weight- and gender-matched stranger mouse (S2) was introduced into the wire cage on the other side of the box. The test mouse was placed in the center chamber and permitted to explore for 10 min. The close interaction times with the S1 mouse and the S2 mouse were recorded to determine the social novelty preference of the test mouse. The mice were tracked and recorded by ANY-maze Video Track 4.98. The preference index (S1 vs. E) was calculated as the ratio of (S1 − E) to (S1 + E), and the preference index (S2 vs. S1) was calculated as the ratio of (S2 − S1) to (S2 + S1).

Nest-Building Test. Mice were placed in separate home cages with fresh bedding 48 h before the test. One hour before lights out, 3-g compressed cotton square nestlet was placed in the cage. The cotton (>0.1 g) that was not used for nesting was weighed the next morning, and the nests built by the mice were scored as follows: 1) mice did not touch the cotton at all; 2) part of the cotton was torn up (50% to 90% was still intact); 3) cotton was mostly torn up but there was no clearly formed nest; 4) a shaped nest was present but it was loose and flat; and 5) a well-identified nest with the wall higher than the mouse was made.

Sucrose Preference Test. The mice were individually housed with ad libitum access to food and water. One week later, the normal water bottles were replaced with two bottles of the same appearance, color, and volume filled with 1% sucrose. To eliminate the mouse's preference for the location and type of water bottle, the location of the bottles was switched after 24 h, and the amount of sugar water consumed within 48 h was weighed and calculated. The two bottles of sugar water were replaced with normal drinking water, the positions of bottles were switched after 24 h, and the water consumed from the two bottles within 48 h was weighed and calculated. The two bottles of drinking water were replaced with one bottle of 1% sucrose and a new bottle of normal drinking water, and the location of bottles were switched after 24 h. The total consumption of each solution was determined by weighing, and the sugar water preference within 48 h was calculated as follows: sugar water preference (%) = [sugar water consumption / (sugar water consumption + water consumption)] * 100.

Y-Maze Test. The Y-maze apparatus is a three-arm maze shaped like a capital "Y". The mice were placed facing a specific arm and allowed to explore freely in the chamber for 8 min, while their movements in and out of each arm were recorded. The correct alternation was calculated as follows: correct alternation % = [(number of consecutive entries into three arms/(total number of entries-2) * 100.

Drug Administration. Risperidone (0.05 mg/kg/d, R3030, Sigma-Aldrich) was administered 1 h before the behavioral test. MK-801 [(+)-MK-801 hydrogen maleate, M107, Sigma-Aldrich, 0.2 mg/kg] was administered by i.p. injection once daily starting 2 wk before behavioral tests. Amthamine (ab120778, Abcam, 1 mM, 500 nL), betazole (HY-B1557, MedChemExpress, 10 mM, 500 nL), or ZD7288 (ab120102, Abcam, 1 mM, 500 nL) was administrated into two sides of the mPFC via cannulas 30 min before the test.

Virus Injection and Cannula Implantation. Histamine H_2R was Cre-dependently knocked down using *AAV-FLEX-shHrh2-GFP* (*AAV-FLEX-scramble shRNA-GFP* as a control virus) and overexpressed using *AAV-FLEX-Hrh2-GFP* (*AAV-FLEX-neg-GFP* as a control virus) produced by OBiO Technology. Mice were anesthetized by sodium pentobarbital (50 mg/kg, i.p.) and restrained by a stereotaxic apparatus (RWD Life Science). The viruses were injected into the mPFC (500 nL, 10 min; AP +1.9 mm, ML ± 0.4 mm, DV −2.3 mm) and hippocampus (200 nL, 10 min; AP −2.9 mm, ML ± 3.2 mm, DV −3.2 and −2.5 mm). Mice were raised for 3 wk to ensure virus expression after surgery. The regions of the mice injected with the virus were tested for expression, and those mice injected in the wrong location were eliminated. For intra-mPFC injection, bilateral cannulas were implanted into the mPFC (AP + 1.9 mm, ML ± 0.4 mm, DV −2.3mm) 1 wk before the amthamine, betazole, or ZD7288 administration and behavioral tests.

In Situ Hybridization by RNAscope. Mice were perfused with 4% paraformaldehyde (PFA), and then brains were fixed in 4% PFA overnight and dehydrated in 30% sucrose for the next 2 d. Frozen brain slices with 14-μm thickness were subjected to in situ hybridization. The RNAscope Multiplex Fluorescent Reagent Kit v2 (323100, Advanced Cell Diagnostics) was used for checking *Hrh2* expression or duplex hybridization using the *Hrh2* probe (517751, Advanced Cell Diagnostics, C1) with a *GFP* probe (400281, Advanced Cell Diagnostics, C2) and a *CaMKIIα* probe (445231, Advanced Cell Diagnostics, C3). For human post-mortem brain tissues, 8-μm thickness paraffin embedded slices were subjected to in situ hybridization with the RNAscope Multiplex Fluorescent Reagent Kit v2 using the *Hrh2* probe (416511, Advanced Cell Diagnostics), and then incubated with anti-glutamate (G6642, Sigma-Aldrich, 1:1,000) for double labeling using a combination of in situ hybridization and immunofluorescence. Fluorescence images were photographed by a Leica SP8 laser confocal microscope.

Single-Unit Recording and Analysis. Mice were anesthetized with urethane (1.2 g/kg) and their neuronal activity was recorded by an eight-wire bundle of microelectrodes (12 μm, AM-Systems) with an impedance of 1 to 2 MΩ. Neuronal activity was sampled by the Cerebus acquisition system and analyzed by offline sorting software (Plexon) (61).

Electrophysiology. The mice were quickly perfused with ice-cold artificial cerebrospinal fluid (ACSF) containing 120 mM NaCl, 2.5 mM KCl, 11 mM glucose, 1.28 mM $MgSO_4$, 3.3 mM $CaCl_2$, 1 mM NaH_2PO_4, and 14.3 mM $NaHCO_3$ (Sigma-Aldrich). The brain was quickly transferred to a vibratome (VT1000 mol/L/E, Leica) to prepare 300-μm-thick coronal slices before being incubated in ACSF bubbled with 95% O_2 and 5% CO_2 for 1 min. Then the prepared coronal slices containing the mPFC were recovered in a chamber filled with ACSF and saturated with 95% O_2 and 5% CO_2 at 37 °C for 30 min, and incubated at room temperature for 1 h before recording. Patch pipettes with resistances ranging from 5 to 10 MΩ and filled with recording solution (5 mM NaCl, 140 mM K-gluconate, 0.2 mM EGTA, 2 mM Mg-ATP and 10 mM HEPES, Sigma-Aldrich) were used for patch clamping. Intrinsic action potential firing frequency was calculated using a 0 to 180 pA depolarizing step current with 20 pA increments under the current-clamp mode. To measure the HCN channel activity, we used the voltage-clamp mode and generated the I_h current by applying a −130 mV to −60 mV hyperpolarizing step voltage. ZD7288 (50 μM) was added to the ACSP and applied to the incubation of brain slices. Signals were amplified and recorded by an HEKA EPC10 amplifier (HEKA Instruments, Germany).

Statistics. All data were collected and analyzed in a blinded way. Data are presented as the mean ± SEM. Two groups were compared by an unpaired Student's *t* test, and three or more groups were statistically compared by ANOVA tests, if they fit the normal distribution. In case of non-normal data distribution, Mann–Whitney *U* test was used for single comparisons, and Kruskal–Wallis test was used for one-way analysis of variance. Prism (version 9.0) was used for statistical analyses. The statistical significance threshold was set at 0.05, and significance levels are presented as $*P \leq 0.05$, $**P \leq 0.01$, and $***P \leq 0.001$ in all figures. See also Dataset S1 for further statistical information.

Data, Materials, and Software Availability. All study data are included in the article and/or *SI Appendix*.

ACKNOWLEDGMENTS. This work was supported by the National Natural Science Foundation of China (81973302), National Key R&D Program of China (No. 2020YFA0803900), and Starry Night Science Fund of Zhejiang University Shanghai Institute for Advanced Study (Grant No. SN-ZJU-SIAS-0011). We thank Sanhua Fang, Li Liu and Daohui Zhang from the Core Facilities, Zhejiang University School of Medicine for their technical support.

Author affiliations: [a]Department of Pharmacology, the Second Affiliated Hospital, Key Laboratory of Medical Neurobiology of the Ministry of Health of China, School of Basic Medical Sciences, Zhejiang University School of Medicine, Hangzhou 310058, China; and [b]Key Laboratory of Neuropharmacology and Translational Medicine of Zhejiang Province, Zhejiang Chinese Medical University, Hangzhou 310053, China

Author contributions: Q.M., L.J., X.Z., Yi Wang, Z.C., and W.H. designed research; Q.M., L.J., H.C., and Y.P. performed research; H.D., X.Z., Yi Wang, Z.C., and W.H. contributed new reagents/analytic tools; Q.M., L.J., D.A., Y.P., Yujia Wang, Z.C., and W.H. analyzed data; and Q.M., L.J., Z.C., and W.H. wrote the paper.

1. R. A. McCutcheon, A. Abi-Dargham, O. D. Howes, Schizophrenia, dopamine and the striatum: From biology to symptoms. *Trends Neurosci.* **42**, 205–220 (2019).
2. M. Huhn *et al.*, Comparative efficacy and tolerability of 32 oral antipsychotics for the acute treatment of adults with multi-episode schizophrenia: a systematic review and network meta-analysis. *Lancet* **394**, 939–951 (2019).
3. Q. Wu *et al.*, Developments in biological mechanisms and treatments for negative symptoms and cognitive dysfunction of schizophrenia. *Neurosci. Bull.* **37**, 1609–1624 (2021).
4. G. Lee, Y. Zhou, NMDAR hypofunction animal models of schizophrenia. *Front. Mol. Neurosci.* **12**, 185 (2019).
5. M. Laruelle, Schizophrenia: From dopaminergic to glutamatergic interventions. *Curr. Opin. Pharmacol.* **14**, 97–102 (2014).
6. R. R. Girgis, A. W. Zoghbi, D. C. Javitt, J. A. Lieberman, The past and future of novel, non-dopamine-2 receptor therapeutics for schizophrenia: A critical and comprehensive review. *J. psychiatric Res.* **108**, 57–83 (2019).
7. A. Egerton *et al.*, Glutamate in schizophrenia: Neurodevelopmental perspectives and drug development. *Schizophr. Res.* **223**, 59–70 (2020).
8. W. Hu, Z. Chen, The roles of histamine and its receptor ligands in central nervous system disorders: An update. *Pharmacol. Therapeutics* **175**, 116–132 (2017).
9. P. Panula, S. Nuutinen, The histaminergic network in the brain: Basic organization and role in disease. *Nat. Rev. Neurosci.* **14**, 472–487 (2013).
10. G. D. Prell *et al.*, Histamine metabolites in cerebrospinal fluid of patients with chronic schizophrenia: Their relationships to levels of other aminergic transmitters and ratings of symptoms. *Schizophr. Res.* **14**, 93–104 (1995).
11. L. Cheng *et al.*, Histamine H1 receptor deletion in cholinergic neurons induces sensorimotor gating ability deficit and social impairments in mice. *Nat. Commun.* **12**, 1142 (2021).
12. S. Wu, C. Gao, F. Han, H. Cheng, Histamine H1 receptor in basal forebrain cholinergic circuit: A novel target for the negative symptoms of schizophrenia? *Neurosci. Bull.* **38**, 558–560 (2022).
13. U. Knigge, J. Warberg, The role of histamine in the neuroendocrine regulation of pituitary hormone secretion. *Acta Endocrinol.* **124**, 609–619 (1991).
14. U. Knigge, J. Warberg, Neuroendocrine functions of histamine. *Agents Actions Suppl.* **33**, 29–53 (1991).
15. M. B. Passani *et al.*, Histamine regulates memory consolidation. *Neurobiol. Learn Mem.* **145**, 1–6 (2017).
16. J. S. Bonini *et al.*, Histamine facilitates consolidation of fear extinction. *Int. J. Neuropsychopharmacol.* **14**, 1209–1217 (2011).
17. C. K. da Silveira, C. R. Furini, F. Benetti, C. Monteiro Sda, I. Izquierdo, The role of histamine receptors in the consolidation of object recognition memory. *Neurobiol. Learn Mem.* **103**, 64–71 (2013).
18. L. Jiang *et al.*, Histamine H2 receptor negatively regulates oligodendrocyte differentiation in neonatal hypoxic-ischemic white matter injury. *J. Exp. Med.* **218** (2021).
19. R. B. Rosse *et al.*, An open-label study of the therapeutic efficacy of high-dose famotidine adjuvant pharmacotherapy in schizophrenia: Preliminary evidence for treatment efficacy. *Clin. Neuropharmacol.* **19**, 341–348 (1996).
20. V. S. Mehta, D. Ram, Role of ranitidine in negative symptoms of schizophrenia–an open label study. *Asian J. Psychiatry* **12**, 150–154 (2014).
21. T. Kishi, N. Iwata, Efficacy and tolerability of histamine-2 receptor antagonist adjunction of antipsychotic treatment in schizophrenia: A meta-analysis of randomized placebo-controlled trials. *Pharmacopsychiatry* **48**, 30–36 (2015).
22. P. P. Orange *et al.*, Individuals with schizophrenia have an increased incidence of the H2R649G allele for the histamine H2 receptor gene. *Mol. Psychiatry* **1**, 466–469 (1996).
23. Y. Fukushima *et al.*, G649, an allelic variant of the human H2 receptor with low basal activity, is resistant to upregulation upon antagonist exposure. *Pharmacogenomics J.* **1**, 78–83 (2001).
24. N. R. Swerdlow *et al.*, Startle gating deficits in a large cohort of patients with schizophrenia: Relationship to medications, symptoms, neurocognition, and level of function. *Arch. Gen. Psychiatry* **63**, 1325–1335 (2006).
25. A. Mena *et al.*, Reduced prepulse inhibition as a biomarker of schizophrenia. *Front. Behav. Neurosci.* **10**, 202 (2016).
26. B. K. Yee, J. Feldon, Distinct forms of prepulse inhibition disruption distinguishable by the associated changes in prepulse-elicited reaction. *Behav. Brain Res.* **204**, 387–395 (2009).
27. D. L. Filion, M. E. Dawson, A. M. Schell, Modification of the acoustic startle-reflex eyeblink: A tool for investigating early and late attentional processes. *Biol. Psychol.* **35**, 185–200 (1993).
28. M. E. Dawson, E. A. Hazlett, D. L. Filion, K. H. Nuechterlein, A. M. Schell, Attention and schizophrenia: Impaired modulation of the startle reflex. *J. Abnorm Psychol.* **102**, 633–641 (1993).
29. J. P. Kesby, T. H. Burne, J. J. McGrath, D. W. Eyles, Developmental vitamin D deficiency alters MK 801-induced hyperlocomotion in the adult rat: An animal model of schizophrenia. *Biol. Psychiatry* **60**, 591–596 (2006).
30. X. Li, D. Morrow, J. M. Witkin, Decreases in nestlet shredding of mice by serotonin uptake inhibitors: Comparison with marble burying. *Life Sci.* **78**, 1933–1939 (2006).
31. P. D. Harvey, J. B. Rosenthal, Cognitive and functional deficits in people with schizophrenia: Evidence for accelerated or exaggerated aging? *Schizophr Res.* **196**, 14–21 (2018).
32. T. Sigurdsson, Neural circuit dysfunction in schizophrenia: Insights from animal models. *Neuroscience* **321**, 42–65 (2016).
33. M. D. Rubio, J. B. Drummond, J. H. Meador-Woodruff, Glutamate receptor abnormalities in schizophrenia: Implications for innovative treatments. *Biomol. Ther.* **20**, 1–18 (2012).
34. V. Bubenikova-Valesova, J. Horacek, M. Vrajova, C. Hoschl, Models of schizophrenia in humans and animals based on inhibition of NMDA receptors. *Neurosci. Biobehav. Rev.* **32**, 1014–1023 (2008).
35. M. E. Jackson, H. Homayoun, B. Moghaddam, NMDA receptor hypofunction produces concomitant firing rate potentiation and burst activity reduction in the prefrontal cortex. *Proc. Natl. Acad. Sci. U.S.A.* **101**, 8467–8472 (2004).
36. F. Yi *et al.*, Autism-associated SHANK3 haploinsufficiency causes Ih channelopathy in human neurons. *Science* **352**, aaf2669 (2016).
37. C. He, F. Chen, B. Li, Z. Hu, Neurophysiology of HCN channels: From cellular functions to multiple regulations. *Progress Neurobiol.* **112**, 1–23 (2014).
38. G. Coruzzi, H. Timmerman, M. Adami, G. Bertaccini, The new potent and selective histamine H2 receptor agonist amthamine as a tool to study gastric secretion. *Naunyn Schmiedebergs Arch. Pharmacol.* **348**, 77–81 (1993).
39. J. R. Malagelada, G. F. Longstreth, T. B. Deering, W. H. Summerskill, V. L. Go, Gastric secretion and emptying after ordinary meals in duodenal ulcer. *Gastroenterology* **73**, 989–994 (1977).
40. R. Liao *et al.*, Histamine H1 receptors in neural stem cells are required for the promotion of neurogenesis conferred by H3 receptor antagonism following traumatic brain injury. *Stem Cell Rep.* **12**, 532–544 (2019), 10.1016/j.stemcr.2019.01.004.
41. N. L. Roenker *et al.*, Effect of paliperidone and risperidone on extracellular glutamate in the prefrontal cortex of rats exposed to prenatal immune activation or MK-801. *Neurosci. Lett.* **500**, 167–171 (2011).
42. C. J. Carter, Schizophrenia susceptibility genes converge on interlinked pathways related to glutamatergic transmission and long-term potentiation, oxidative stress and oligodendrocyte viability. *Schizophr. Res.* **86**, 1–14 (2006).
43. V. Labrie, J. C. Roder, The involvement of the NMDA receptor D-serine/glycine site in the pathophysiology and treatment of schizophrenia. *Neurosci. Biobehav. Rev.* **34**, 351–372 (2010).
44. T. M. Ballard *et al.*, Severe impairment of NMDA receptor function in mice carrying targeted point mutations in the glycine binding site results in drug-resistant nonhabituating hyperactivity. *J. Neurosci.* **22**, 6713–6723 (2002).
45. V. Labrie, T. Lipina, J. C. Roder, Mice with reduced NMDA receptor glycine affinity model some of the negative and cognitive symptoms of schizophrenia. *Psychopharmacology* **200**, 217–230 (2008).
46. V. M. Tatard-Leitman *et al.*, Pyramidal cell selective ablation of N-methyl-D-aspartate receptor 1 causes increase in cellular and network excitability. *Biol. Psychiatry* **77**, 556–568 (2015).
47. S. M. Holley *et al.*, Frontal cortical synaptic communication is abnormal in Disc1 genetic mouse models of schizophrenia. *Schizophr Res.* **146**, 264–272 (2013).
48. Y. C. Li, C. Kellendonk, E. H. Simpson, E. R. Kandel, W. J. Gao, D2 receptor overexpression in the striatum leads to a deficit in inhibitory transmission and dopamine sensitivity in mouse prefrontal cortex. *Proc. Natl. Acad. Sci. U.S.A.* **108**, 12107–12112 (2011).
49. P. Panula *et al.*, International union of basic and clinical pharmacology. XCVIII. Histamine receptors. *Pharmacol. Rev.* **67**, 601–655 (2015).
50. Q. X. Zhuang *et al.*, Regularizing firing patterns of rat subthalamic neurons ameliorates parkinsonian motor deficits. *J. Clin. Invest.* **128**, 5413–5427 (2018), 10.1172/JCI99986.
51. B. N. van Berckel *et al.*, D-cycloserine increases positive symptoms in chronic schizophrenic patients when administered in addition to antipsychotics: A double-blind, parallel, placebo-controlled study. *Neuropsychopharmacology* **21**, 203–210 (1999).
52. D. Bugarski-Kirola *et al.*, Bitopertin in negative symptoms of schizophrenia-results from the phase III flashLyte and dayLyte studies. *Biol. Psychiatry* **82**, 8–16 (2017).
53. V. L. Stauffer *et al.*, Pomaglumetad methionil: No significant difference as an adjunctive treatment for patients with prominent negative symptoms of schizophrenia compared to placebo. *Schizophr. Res.* **150**, 434–441 (2013).
54. J. T. Kantrowitz, Managing negative symptoms of schizophrenia: How far have we come? *CNS Drugs* **31**, 373–388 (2017).
55. R. Kaminsky, T. M. Moriarty, J. Bodine, D. E. Wolf, M. Davidson, Effect of famotidine on deficit symptoms of schizophrenia. *Lancet* **335**, 1351–1352 (1990).
56. K. Meskanen *et al.*, A randomized clinical trial of histamine 2 receptor antagonism in treatment-resistant schizophrenia. *J. Clin. Psychopharmacol.* **33**, 472–478 (2013).
57. M. Poyurovsky *et al.*, The effect of famotidine addition on olanzapine-induced weight gain in first-episode schizophrenia patients: A double-blind placebo-controlled pilot study. *Eur. Neuropsychopharmacol.* **14**, 332–336 (2004).
58. C. Andrade, Famotidine augmentation in schizophrenia: Hope or hype? *J. Clin. Psychiatry* **74**, e855–e858 (2013).
59. M. Shahid, G. B. Walker, S. H. Zorn, E. H. Wong, Asenapine: A novel psychopharmacologic agent with a unique human receptor signature. *J. Psychopharmacol.* **23**, 65–73 (2009).
60. W. Qiu *et al.*, Standardized operational protocol for human brain banking in China. *Neurosci. Bull.* **35**, 270–276 (2019).
61. Y. Wang *et al.*, Depolarized GABAergic signaling in subicular microcircuits mediates generalized seizure in temporal lobe epilepsy. *Neuron* **95**, 1221 (2017).